

The Fate of a Bimetallic Ethylene Dimerization Catalyst: Synthesis and Structure of $(\text{dfepe})_2\text{Ir}_2(\mu\text{-}\eta^1\text{:}\eta^3\text{-C}_4\text{H}_6)(\mu\text{-H})(\text{H})$ ($\text{dfepe} = (\text{C}_2\text{F}_5)_2\text{PCH}_2\text{CH}_2\text{P}(\text{C}_2\text{F}_5)_2$)

Justin M. Hoerter, R. Chris Schnabel, Patricia A. Goodson, and Dean M. Roddick*

Department of Chemistry, University of Wyoming, P.O. Box 3838, Laramie, Wyoming 82071

Received August 16, 1999

Summary: Solutions of $(\text{dfepe})_2\text{Ir}_2(\mu\text{-H})_3(\text{H})$ (**1**; $\text{dfepe} = (\text{C}_2\text{F}_5)_2\text{PCH}_2\text{CH}_2\text{P}(\text{C}_2\text{F}_5)_2$) react with 1 atm of ethylene at ambient temperatures to catalytically produce a mixture of *trans*- and *cis*-2-butenes and the diiridium methylallyl complex $(\text{dfepe})_2\text{Ir}_2(\mu\text{-}\eta^1\text{:}\eta^3\text{-C}_4\text{H}_6)(\mu\text{-H})(\text{H})$ (**2**).

Introduction

Reactions between metal centers and olefinic substrates are a fundamental component of organometallic chemistry. In addition to olefin dimerization and oligomerization reactions,¹ alkenes have also been effectively used as hydrogen acceptors in hydrogen transfer systems and in the preparation of reactive coordinatively unsaturated metal complexes.² We have previously reported the synthesis and the reactivity properties of a dimeric iridium tetrahydride, $(\text{dfepe})_2\text{Ir}_2(\mu\text{-H})_3(\text{H})$ ($\text{dfepe} = (\text{C}_2\text{F}_5)_2\text{PCH}_2\text{CH}_2\text{P}(\text{C}_2\text{F}_5)_2$).³ This dimer may be formally viewed as a coordinatively saturated Ir(I)/Ir(III) system which may undergo reactions via an unbridged Ir(I)/Ir(III) tetrahydride intermediate (Scheme 1).

The subsequent formation of a highly reactive dihydride dimer, $(\text{dfepe})_2\text{Ir}_2(\mu\text{-H})_2$, was proposed by us both in alkane dehydrogenation reactions by $(\text{dfepe})_2\text{Ir}_2(\mu\text{-H})_3(\text{H})$ and in the deprotonation of $(\text{dfepe})_2\text{Ir}_2(\mu\text{-H})_2(\mu\text{-O}_3\text{SCF}_3)$.^{3,4} In a further effort to directly access this species, we have examined reactions of $(\text{dfepe})_2\text{Ir}_2(\mu\text{-H})_3(\text{H})$ with ethylene as a hydrogen scavenger. We report here that simple dehydrogenation is not observed. Instead, $(\text{dfepe})_2\text{Ir}_2(\mu\text{-H})_3(\text{H})$ functions as a catalyst of limited stability for ethylene dimerization and ultimately undergoes conversion to an unusual allyl-bridged product.

Results and Discussion

Benzene solutions of $(\text{dfepe})_2\text{Ir}_2(\mu\text{-H})_3(\text{H})$ (**1**) react readily with 1 atm of ethylene at ambient temperatures. After 2 h, a mixture of *trans*- and *cis*-2-butenes (2.7:1) was produced, along with a 20% conversion of **1** to a new dimeric iridium species, **2** (Scheme 2). Small

amounts (<0.5 equiv) of ethane were observed by ¹H NMR during the course of this reaction. The initial catalytic ethylene dimerization activity of this system was estimated to be 0.7 turnover h⁻¹; over time this activity diminished, concomitant with the formation of **2**. No reaction was observed at 20 °C when $(\text{dfepe})_2\text{Ir}_2(\mu\text{-H})_3(\text{H})$ (**1**) was treated with 1 atm of tetrafluoroethylene.

The preliminary spectroscopic data did not uniquely establish the identity of **2**. Complex unresolved (1:1:1) vinylic resonances are observed by ¹H NMR (benzene-*d*₆) at 8.68, 3.95, and 3.16 ppm. In addition, 1:1 broad hydride resonances appear at -8.91 and -15.81 ppm which are characteristic of terminal and bridging coordination, respectively, for this family of compounds. The broadness of these hydride signals is due to unresolved *J*_{HF} coupling with the dfepe C₂F₅ groups. A $\mu\text{-}\eta^1\text{:}\eta^2\text{-CH=CH}_2$ bridging vinyl formulation similar to that in previously reported rhodium systems⁵ was initially considered; however, additional experiments revealed that both 1- and 2-butenes also react cleanly with **1** to form **2**. Closer examination of ¹H spectra and homonuclear COSY data confirmed the presence of a vinyl-coupled methyl resonance at 1.80 ppm. These observations, together with ¹³C NMR data and a subsequent structural determination by X-ray diffraction (vide infra), confirmed the presence of a $\mu\text{-}\eta^1\text{:}\eta^3\text{-C}_4\text{H}_6$ methylallyl fragment in the diiridium complex **2**.

Complex **2** is catalytically inactive toward further ethylene dimerization, but both **1** and **2** serve as olefin isomerization catalysts. At ambient temperature, 1-butene, *cis*-2-butene, and *trans*-2-butene all convert completely to a thermodynamic mixture of *cis*- and *trans*-2-butenes and a trace amount of 1-butene after 24 h. Both **1** and **2** also function as olefin hydrogenation catalysts: conversion of 1- and 2-butenes under H₂ in the presence of either **1** or **2** to butane under ambient conditions is complete within 15 min. Consistent with this, hydrogenation of the methylallyl-bridged dimer quantitatively produces the tetrahydride parent complex and 1 equiv of butane at a comparable rate. In a competition experiment, equal amounts (~2 atm) of ethylene and hydrogen gas were added to a benzene solution of **1** at ambient temperature. After 15 min an ~10% conversion to the allyl-bridged dimer **2** occurred,

(1) Keim, W.; Behr, A.; Roper, M. In *Comprehensive Organometallic Chemistry*; Wilkinson, G., Stone, F. G. A., Abel, E. W., Eds.; Pergamon: New York, 1982; Vol. 8, p 371.

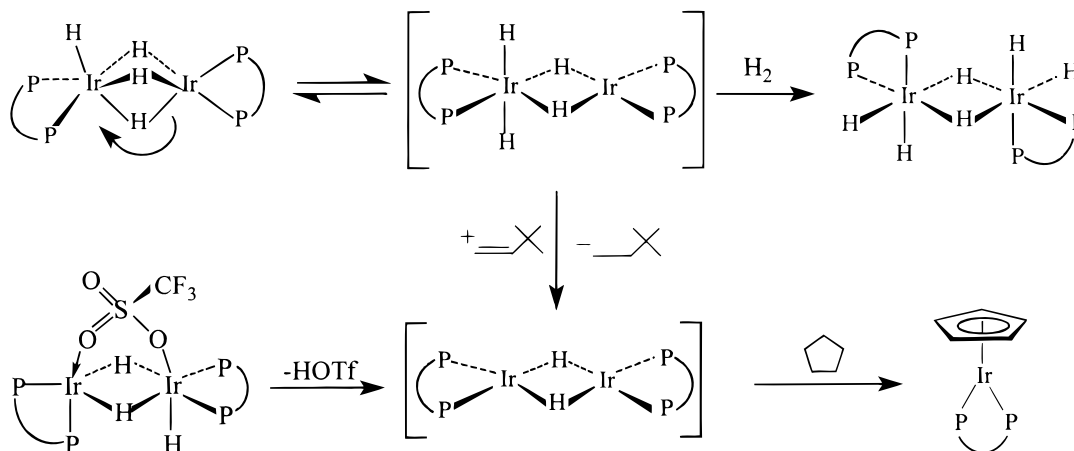
(2) Fuchen, L.; Pak, E. B.; Singh, B.; Jensen, C. M.; Goldman, A. S. *J. Am. Chem. Soc.* **1999**, *121*, 4086 and references therein.

(3) Schnabel, R. C.; Carroll, P. S.; Roddick, D. M. *Organometallics* **1996**, *15*, 655.

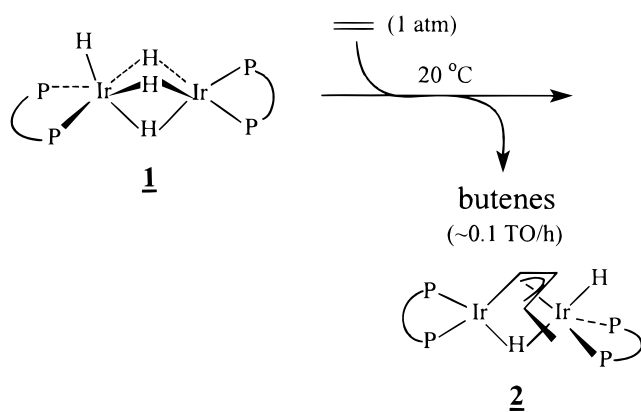
(4) Schnabel, R. C.; Roddick, D. M. *Organometallics* **1993**, *12*, 704.

(5) Fryzuk, M. D.; Jones, T.; Einstein, F. W. B. *Organometallics* **1984**, *3*, 185.

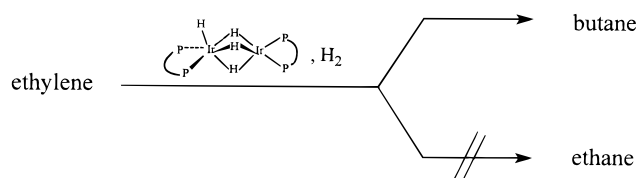
Scheme 1



Scheme 2



Scheme 3



and the primary initial organic product was *cis*-2-butene with only a trace of ethane. In the presence of excess H₂, butane and **1** are the principal products observed (Scheme 3). Thus, under these conditions the dimerization of ethylene is kinetically preferred over hydrogenation in this particular system.

Structural Determination of (dfepe)₂Ir₂(μ-η¹:η³-C₄H₆)(μ-H)(H) (2). A suitable yellow prism of **2** was grown by slow evaporation from dichloromethane, and the solid-state structure was determined by X-ray diffraction at -100 °C; selected data collection and metrical data are presented in Tables 1 and 2, and views of the structure are given in Figures 1 and 2. With the exception of positional disorder in one of the dfepe C₂F₅ units (see Experimental Section), a satisfactory refinement was obtained. The most distinctive feature of this structure is the μ-η¹:η³ coordination of the methylallyl group. The allyl carbon bond distances to Ir(2) of the bridge (C(21)–Ir(2) = 2.202(7) Å) and central carbon (C(22)–Ir(2) = 2.209(6) Å) are significantly shorter than the terminal distance (C(23)–Ir(2) = 2.267(7) Å) and are essentially identical with the η³-allyl coordination parameters for the previously reported Ir(III) complex

Table 1. Crystallographic Data for (dfepe)₂Ir₂(μ-η¹:η³-C₄H₆)(μ-H)(H) (2)

chem formula	C ₂₄ H ₁₄ F ₄₀ Ir ₂ P ₄	space group	$P\bar{1}$ (No. 2)
fw	1570.63	V (Å ³)	2081.5(5)
a (Å)	11.5987(14)	Z	2
b (Å)	12.603(2)	λ (Å)	0.710 73
c (Å)	15.517(2)	T (°C)	-100
α (deg)	67.733(8)	ρ_{calcd} (g cm ⁻³)	2.506
β (deg)	82.646(9)	$R1$ (all data) ^a	0.0461
γ (deg)	86.304(10)		

$$^a R1 = \sum(|F_o| - |F_c|) / \sum |F_o|.$$

Table 2. Selected Bond Lengths (Å) and Angles (deg) for (dfepe)₂Ir₂(μ-η¹:η³-C₄H₆)(μ-H)(H) (2)

Ir(1)–P(1)	2.148(2)	Ir(1)–P(2)	2.206(2)
Ir(1)–C(21)	2.081(7)	Ir(2)–P(3)	2.226(2)
Ir(2)–P(4)	2.225(2)	Ir(2)–C(21)	2.202(7)
Ir(2)–C(22)	2.209(6)	Ir(2)–C(23)	2.267(7)
C(21)–C(22)	1.396(10)	C(22)–C(23)	1.420(10)
C(23)–C(24)	1.508(10)		
P(1)–Ir(1)–P(2)	84.69(7)	P(3)–Ir(2)–P(4)	85.86(7)
P(1)–Ir(1)–Ir(2)	146.13(5)	P(2)–Ir(1)–Ir(2)	128.87(5)
P(1)–Ir(1)–C(21)	96.6(2)	P(3)–Ir(2)–Ir(1)	104.48(5)
P(4)–Ir(2)–Ir(1)	126.49(6)	P(3)–Ir(2)–C(21)	103.8(2)
P(3)–Ir(2)–C(22)	128.9(2)	P(3)–Ir(2)–C(23)	165.3(2)
P(4)–Ir(2)–C(21)	168.9(2)	P(4)–Ir(2)–C(22)	138.5(2)
P(4)–Ir(2)–C(23)	105.6(2)	C(21)–C(22)–C(23)	119.5(6)
C(22)–C(23)–C(24)	119.7(7)		

(dfepe)Ir(η³-C₃H₅)(H)(OTf).⁶ The bridging allyl carbon C(21) is coplanar with Ir(1), P(1), and P(2) and *trans* (178.6°) with respect to P(2). The observed Ir–Ir bond distance of 2.8679(6) Å is significantly longer than those of (dfepe)₂Ir₂(μ-H)₃(H) (2.536(3) Å) and [(dfepe)Ir(μ-H)(H)₂]₂ (2.703(2) Å) but is closely comparable to Ir–Ir distances reported for other μ-η¹:η³ allyl structures.⁷

The hydride ligands in **2** were not located on residual electron density maps. However, the plane defined by P(1), P(2), and Ir(1) is essentially coincident with the Ir(1)Ir(2)C(21) plane (4.7°) and is consistent with a square-planar coordination geometry about Ir(1) with a bridging hydride ligand *trans* to P(1). The location of the terminal hydride is not obvious from the disposition of the two planes defined by Ir(1)P(1)P(2) and Ir(2)–P(3)P(4) or the position of the allyl group. The lack of any significant ²J_{PH} or ²J_{HH} coupling to the hydride resonance at -15.81 ppm suggests that it is likely *cis*

(6) Schnabel, R. C.; Roddick, D. M. *Organometallics* **1996**, *15*, 3550.

(7) McGhee, W. D.; Hollander, F. J.; Bergman, R. G. *J. Am. Chem. Soc.* **1988**, *110*, 8428.

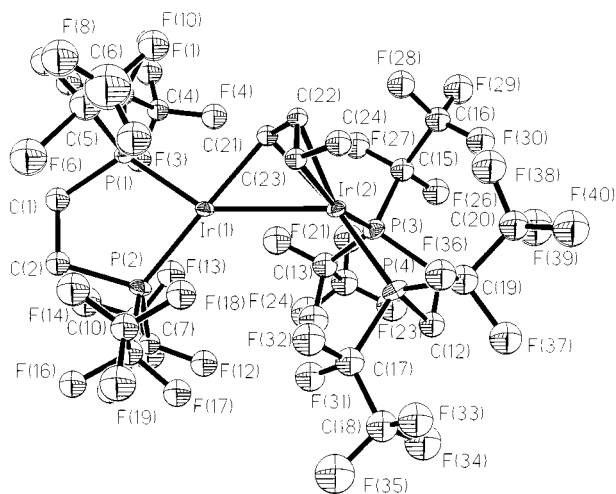


Figure 1. Molecular structure of $(dfep)_2Ir_2(\mu-H)(\mu-\eta^3-C_4H_6)$ (**2**) with atom-labeling scheme (30% probability ellipsoids).

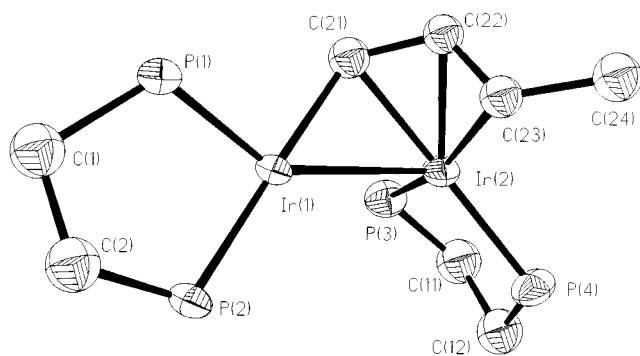


Figure 2. View of the $Ir_2(\mu-\eta^3-C_4H_6)$ framework of **2** (50% probability ellipsoids).

to the phosphorus ligands on either Ir(1) or Ir(2). Proton–phosphorus correlation NMR experiments did not furnish an unambiguous assignment of the terminal hydride to either iridium center. Since the allyl centroid is only slightly displaced (2.1°) from the vector bisecting the Ir(2)–P(3) and Ir(2)–P(4) bonds and the Ir(1)Ir(2)–C(21) plane is tilted only 4.7° away from the Ir(1)P(1)–P(2) plane (away from the allyl group), there is no clear void space assignable to the terminal hydride on either Ir(1) or Ir(2). Nevertheless, we have depicted **2** as having the terminal hydride ligand on the η^3 -allyl-coordinated iridium, corresponding to a localized bonding description where Ir(1) may be described as a four-coordinate Ir(I) complex, $(dfep)Ir(\text{alkyl})(L)$, and Ir(2) as a coordinatively saturated Ir(III) complex, $(dfep)Ir(\text{allyl})(H)_2$. We have previously reported a similar Ir(III) allyl hydride complex, $(dfep)Ir(\eta^3-C_3H_5)(H)(OTf)$.⁶

Any mechanism which accounts for both olefin dimerization and the ultimate formation of **2** from **1** is purely speculative in the absence of additional data. As is often the case for polymetallic systems, a complication exists regarding the molecularity of the active dimerization catalyst. Nevertheless, the fact that treatment of **1** by either ethylene or butenes cleanly yields **2**, together with the robust nature of the tetrahydride dimer, suggests that a common butyl bimetallic intermediate may be involved, although a monomeric intermediate such as $(dfep)Ir(Et)(\eta^2-C_2H_4)$ is also a possibility. A bimetallic butyl intermediate may subsequently undergo either

β -elimination to form butene products or allylic C–H activation which irreversibly (in the absence of added H_2) leads to the final methylallyl product **2**.

Experimental Section

General Procedures. All manipulations were conducted under an atmosphere of purified nitrogen using high-vacuum and/or glovebox techniques. Dry oxygen-free solvents were prepared using standard procedures. Aprotic deuterated solvents used in NMR experiments were dried over activated 3 Å molecular sieves. Elemental analyses were performed by Desert Analytics. IR spectra were recorded on a Bomem MB-100 instrument as Nujol mulls using NaCl plates. NMR spectra were obtained on a Bruker Avance 400 instrument. ³¹P spectra were referenced to an 85% H_3PO_4 external standard. $(dfep)_2Ir_2(\mu-H)_3(H)$ was prepared using the previously described method.³

$(dfep)_2Ir_2(\mu-\eta^3-\eta^1-C_4H_6)(\mu-H)(H)$ (2**).** A solution of 0.200 g (0.132 mmol) of $(dfep)_2Ir_2(\mu-H)_3(H)$ in 30 mL of benzene was stirred under 1 atm of ethylene. After 20 h, the volatiles were removed from the resulting orange solution, and the residue was extracted with petroleum ether and cooled to $-78^\circ C$. Cold filtration of the precipitate afforded 0.186 g (89.9%) of light orange **2**. Anal. Calcd for $C_{24}H_{16}F_{40}Ir_2P_4$: C, 18.33; H, 1.03. Found: C, 18.49; H, 1.06. IR (cm^{-1}): 1305 s, 1238 vs, 1208 s, 1152 s, 1127 s, 1037 w, 972 s, 876 w, 809 w, 751 s. ¹H NMR (acetone- d_6 , 400.12 MHz, $27^\circ C$): δ 8.20 (m, 1H; IrCHCHCHCH₃), 7.29 (m, 1H; IrCHCHCHCH₃), 3.48 (m, 1H; IrCHCHCHCH₃), 2.24 (m, 8H; PCH₂), 1.80 (m, 3H; IrCHCHCHCH₃), -8.91 (br d, $^2J_{PH}(\text{trans}) = 57$ Hz, 1H; Ir($\mu-H$)), -15.81 (m, 1H; Ir(H)). ¹³C{¹H} NMR (acetone- d_6 , 100.62 MHz, $27^\circ C$): δ 129.0 (br d, $^2J_{CP} = 97.0$ Hz), 119.5 (qm, $^1J_{CF} = 287$ Hz; PCF₂CF₃), 110.4 (tm, $^1J_{CF} = 299$ Hz; CF₂), 105.0 (s), 55.2 (d, $^3J_{CP} = 28$ Hz), 24.4 (m; PCH₂), 20.7 (s). ¹⁹F NMR (acetone- d_6 , 376.46 MHz, $27^\circ C$): δ -75.39 , -75.46 , -76.05 , -76.24 , -76.71 , -76.87 , -77.45 , -78.27 (s; PCF₂CF₃), -104 to -118.3 (overlapping ABX multiplets; PCF₂CF₃). ³¹P NMR (acetone- d_6 , 161.99 MHz, $27^\circ C$): δ 83.86 (m), 72.45 (m), 67.99 (m), 64.80 (m).

NMR Experiments. Ethylene dimerization, butene isomerization, and hydrogenation experiments were monitored by ¹H NMR spectroscopy. In a typical experiment, a 5 mm NMR tube was charged with 25 mg of complex **1** in 0.5 mL of benzene- d_6 under nitrogen. Aliquots of dihydrogen and ethylene (4.0 mL) were added sequentially via syringe, and the progress of the reaction was quantified by integration of ¹H NMR spectra.

Crystal Structure Data for 2. Single-crystal X-ray data for $(dfep)_2Ir_2(\mu-\eta^3-\eta^1-C_4H_6)(\mu-H)(H)$ were collected at $-100^\circ C$ using a yellow prism of dimensions $0.40 \times 0.20 \times 0.20$ mm on a Siemens P4 diffractometer. A triclinic cell was determined using the measured positions of 31 reflections in the 2θ range of 9 – 25° . A total of 8359 reflections were gathered, the octants collected being $\pm h, \pm k, +l$, using ω scans in the 2θ range 3.6 – 50° . The data were integrated and averaged to yield 7107 independent reflections.

The structure was solved by direct methods and refined by full-matrix least-squares techniques on F^2 using structure solution programs from the SHELXTL system.⁸ The compound crystallized in the centrosymmetric triclinic space group $P\bar{1}$ ($Z = 2$). Non-hydrogen atoms were refined anisotropically, except for the C5 and C6 perfluoroethyl carbons, which were each disordered between two positions labeled A and B with statistical 1:1 occupancy ratios. C5A, C5B, C6A, and C6B were refined isotropically. Two of the three fluorines attached to C6A share the same positions with two fluorines (F8 and F9) attached to C6B. The third fluorine on C6A shares the same

(8) Sheldrick, G. M. SHELXTL Crystallographic System, version 5.03/Iris; Siemens Analytical X-ray Instruments, Inc., Madison, WI, 1994.

position with F6, a fluorine attached to C5B, while the third fluorine on C6B shares the same position with F10, a fluorine attached to C5A. Hydrogen atoms were refined with fixed isotropic thermal parameters. Allyl hydrogens H21, H22, and H23 were located in the Fourier map, while all other hydrogen atoms were placed in calculated positions. The final R factor values were $R1 = 0.0410$ and $wR2 = 0.1177$ for 6337 data with $F > 4\sigma F$ ($R1 = 0.0461$ and $wR2 = 0.1243$ for 7105 data giving a data-to-parameter ratio of 11:1 and a goodness of fit on F^2 of 1.03). The structure could not be refined successfully using data from a ψ -scan absorption correction; therefore, the data were corrected for absorption using the program XABS2.⁹ The

(9) Parkin, S.; Moezzi, B.; Hope, H. *J. Appl. Crystallogr.* **1995**, *28*, 53.

maximum and minimum residual densities remaining were 1.5 and $-2.2 \text{ e } \text{\AA}^{-3}$, respectively.

Acknowledgment. This work has been supported by the National Science Foundation (Grant CHE-9615985), the Wyoming DOE-EPSCoR Program, and the donors of the Petroleum Research Fund, administered by the American Chemical Society.

Supporting Information Available: A complete listing of data collection and metrical parameters for complex **2**. This material is available free of charge via the Internet at <http://pubs.acs.org>.

OM990659H